THE UNIVERSITY of EDINBURGH

Edinburgh Research Explorer

Characterisation of Microparticles with driven Optical Tweezers

Citation for published version:
Wood, T, Bartlett, P, Roberts, GS & Eaimkhong, S 2008, 'Characterisation of Microparticles with driven Optical Tweezers', Faraday Discussions, vol. 137, pp. 319-333. https://doi.org/10.1039/b703994h

Digital Object Identifier (DOI):
10.1039/b703994h

Link:
Link to publication record in Edinburgh Research Explorer

Document Version:
Publisher's PDF, also known as Version of record

Published In:
Faraday Discussions

General rights
Copyright for the publications made accessible via the Edinburgh Research Explorer is retained by the author(s) and / or other copyright owners and it is a condition of accessing these publications that users recognise and abide by the legal requirements associated with these rights.

Take down policy
The University of Edinburgh has made every reasonable effort to ensure that Edinburgh Research Explorer content complies with UK legislation. If you believe that the public display of this file breaches copyright please contact openaccess@ed.ac.uk providing details, and we will remove access to the work immediately and investigate your claim.

Download date: 24. Oct. 2019

View Article Online / Journal Homepage / Table of Contents for this issue

Characterization of microparticles with driven optical tweezers†

Tiffany A. Wood, G. Seth Roberts, Sarayoot Eaimkhong and Paul Bartlett*

Received 16th March 2007, Accepted 3rd April 2007
First published as an Advance Article on the web 16th July 2007
DOI: 10.1039/b703994h

Published on 16 July 2007. Downloaded by University of Edinburgh on 01/11/2013 20:16:05.

We discuss how actively-driven optical tweezers may be used to characterize Brownian microparticles. Two experiments are described in detail. We follow the thermal fluctuations of a charged particle in an oscillatory electric field and demonstrate that charges as low as a few elementary charges can be measured accurately and reproducibly. Secondly, we measure the orientational dynamics of a trapped rotating droplet and use circular polarimetry within optical tweezers to determine *in situ* birefringence.

1. Introduction

One of the distinctive features of many micro-particulate systems is their diversity—no two particles have precisely the same size, charge or optical properties. Recent advances in soft matter that allow the interactions between individual pairs of microparticles to be studied have spawned an increased interest in characterizing the optical and electrical properties of single microparticles. Single particle detection and imaging offers the promise of new insights into many fundamental physical processes and a better understanding of the functionality of soft matter systems. This information is frequently obscured by ensemble measurements that provide only average material properties.

In this paper, we detail a general approach that utilizes the change in the random walk of a submicron particle following the application of a periodic perturbation to probe the optical and electrical properties of a single microparticle. The way in which the random Brownian motion of a small sphere immersed in a fluid is modified by an external force lies at the core of many diverse problems in physics, chemistry and biology. Examples include the operation of molecular motors,[1] the phenomenon of stochastic resonance[2] and the driven transport of colloids through a potential landscape.[3] We employ a focused laser beam to confine a microparticle in an optical trap and then track the Brownian fluctuations of the trapped particles with nanometer resolution.[4] In the harmonic potential well, generated by the laser beam, the microparticle oscillates around its equilibrium position as a consequence of the random thermal motion of the solvent molecules. By measuring the subsequent changes in these fluctuations produced by external periodic forces, the optical and electrical properties of single microparticles are derived. We analyze the effects of

School of Chemistry, University of Bristol, Bristol, UK BS8 1TS. E-mail: p.bartlett@bristol.ac.uk

† The HTML version of this article has been enhanced with colour images.

View Article Online

two classes of external perturbations: an *oscillatory linear force*, produced by applying an alternating electric field to a charged particle, and a *constant optical torque*, generated by illuminating a spherical birefringent microparticle with circularly-polarized light. The absolute value of the charge and the birefringence of a single microparticle are found from the autocorrelation of the particle's coordinates. We present a detailed analysis of the Brownian fluctuations of the trapped particle in each of these two situations and show how our measurements provide new quantitative tools for characterization of the optical and electrical properties of micrometric systems.

The paper is organised as follows: Section 2 describes the basis of the optical tweezers technique, in Section 3 we place a trapped particle in an oscillatory electric field and use the response to determine the charge on the particle, and in Section 4 we apply a constant angular torque to a trapped particle and record its orientational dynamics.

2. Optical tweezers

Optical tweezers are formed by tightly focusing a laser beam with a high numerical aperture objective lens.[5] The operation of the trap is based on the fact that a dielectric material subject to an external electric field **E** is polarized and generates an induced dipole moment per unit volume, **P**, given by $\mathbf{P} = \chi\mathbf{E}$, where χ is the electric susceptibility.[6] For a uniform dielectric sphere of radius a, χ is isotropic and the polarization **P** is parallel to the electric intensity $\mathbf{E}(\mathbf{r}, t)$ and equal to‡,

$$\mathbf{P}(\mathbf{r}, t) = 3n_{\mathrm{m}}^2\varepsilon_0\left(\frac{m^2-1}{m^2+2}\right)\mathbf{E}(\mathbf{r}, t), \tag{1}$$

where n_{m} is the index of refraction of the medium and m is the ratio of the index of refraction of the particle to the medium ($n_{\mathrm{p}}/n_{\mathrm{m}}$). There is no net force on the dipole in the field **E** unless the field is non-uniform such that one end of the dipole is subjected to a greater force than the other. In the *non-uniform* electric field generated at the focus of a laser beam there is an instantaneous gradient force per unit volume on the dielectric of,

$$\mathbf{F}_{\mathrm{g}}(\mathbf{r}, t) = [\mathbf{P}(\mathbf{r}, t)\cdot\nabla]\mathbf{E}(\mathbf{r}, t) = 3n_{\mathrm{m}}^2\varepsilon_0\left(\frac{m^2-1}{m^2+2}\right)\frac{1}{2}\nabla\mathbf{E}^2(\mathbf{r}, t). \tag{2}$$

The time-averaged gradient force that the particle experiences

$$\mathbf{f}_{\mathrm{g}} = \int \mathrm{d}r\langle[\mathbf{P}(\mathbf{r}, t)\cdot\nabla]\mathbf{E}(\mathbf{r}, t)\rangle, \tag{3}$$

is proportional to the intensity gradient and is directed towards the intensity maximum for $m > 1$. As a result, a highly-focused light beam will tend to confine a high refractive index microparticle within its focal volume. The strength of the isotropic optical forces is controlled by the spatial profile of the beam and the size and refractive index of the particle.[7]

Angular trapping occurs in optical tweezers with spherical particles made from materials such as nematic Liquid Crystals (LCs) that are birefringent. In this case, the susceptibility is no longer isotropic and the expression for the polarization **P** must be generalized to

$$\mathbf{P} = \chi_i E_i\hat{\mathbf{i}} + \chi_j E_j\hat{\mathbf{j}} + \chi_k E_k\hat{\mathbf{k}} \tag{4}$$

where $\hat{\mathbf{i}}$, $\hat{\mathbf{j}}$ and $\hat{\mathbf{k}}$ are unit vectors along the principal axes of the liquid crystal and χ_i, χ_j and χ_k are the corresponding susceptibilities. A uniaxial birefringent material, such

‡ Here, by way of illustration, we have assumed that the trapped sphere is much smaller than the wavelength of the trapping laser, *i.e.* $a \ll \lambda$. Particle shape effects are neglected. More complete theories are required when the dimension of the trapped particle is comparable to the wavelength of the trapping laser.

 This journal is © The Royal Society of Chemistry 2007

Published on 16 July 2007. Downloaded by University of Edinburgh on 01/11/2013 20:16:05.

View Article Online

as a nematic LC, can be described by two susceptibilities: an *ordinary* susceptibility, χ_o, for electric fields normal to the optic axis, and an *extraordinary* susceptibility, χ_e, for fields parallel to the optic axis. Choosing the unit vector $\hat{\mathbf{i}}$ parallel to the optic axis gives, $\chi_i = \chi_e$ and $\chi_j = \chi_k = \chi_o$. Since in general a birefringent nematic LC is more polarizable along the director (the extraordinary axis) than the ordinary axes, the electric polarization vector **P** is not parallel to the external electric field **E** but is tilted towards the extraordinary axis. The misalignment of **P** and **E** means that in a *uniform* electric field, a spherical birefringent particle experiences a torque

$$\tau = \int \mathrm{d}\mathbf{r}\mathbf{P}(\mathbf{r}, t) \times \mathbf{E}(\mathbf{r}, t) \tag{5}$$

that tends to align the ordinary axes of the nematic LC drop with the electric field direction. The polarization state of the trapping beam controls the time-dependence of the resulting torque imparted to the trapped particle. In linearly-polarized light, the particle is angularly trapped and aligned along a particular orientation, and a particular particle is always aligned along the same direction whenever trapped. By contrast, in circularly-polarized light, where the plane of polarization rotates continually, a birefringent particle experiences a constant torque and, if free, rotates with a fixed frequency and angular speed.

2.1 Optical configuration

Fig. 1 shows a schematic of our optical tweezers system. A linearly-polarized TEM_{00} mode of a Ytterbium fibre-coupled laser of wavelength $\lambda = 1064$ nm (IPG Photonics, Germany) was focussed to a diffraction-limited beam spot with a diameter of approximately of 0.9 μm by an oil-immersion microscope objective (Plan-Neofluar, ×100, N.A. 1.3, Zeiss) mounted in an inverted microscope (Axiovert S100, Zeiss). The intensity of the laser beam was varied using a combination of a $\lambda/2$ waveplate and a polarizing beam-splitter cube placed in the beam path. For the optical torque experiments an additional $\lambda/4$ plate was placed immediately before the objective to convert the linearly polarized light of the laser into the circularly-polarized beam required to rotate the birefringent particles. The transmitted laser beam and light scattered by the trapped microparticle was collected by a high numerical aperture oil-immersion objective and projected onto a polarizing beam splitting cube, before being sent to two orthogonal quadrant photodetectors (model QD50-4X, Centronics, UK).

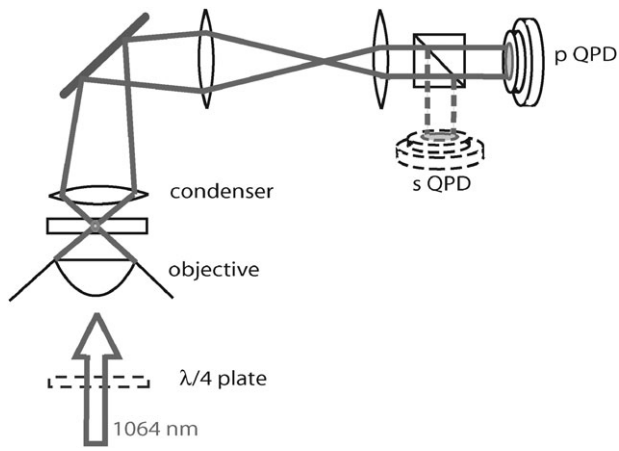

Fig. 1 Schematic representation of the optical tweezer apparatus. Components shown dashed were added for measurements under applied optical torque.

Published on 16 July 2007. Downloaded by University of Edinburgh on 01/11/2013 20:16:05.

View Article Online

The signals from the two orthogonal detectors were analyzed in different ways depending on the optical experiment. In the linear force experiments detailed in Section 3, the in-plane position of the trapped particle was tracked with the resolution of a few nanometers by back-plane optical interferometry.[8] The quadrant photodetectors were aligned so that they recorded the intensity profile of the pattern generated by the interference of scattered and transmitted light in a plane conjugate to the focal plane. Appropriate combinations of the four quadrant signals give a voltage proportional to the instantaneous in-plane x and y displacement of the fluctuating particle, relative to the axis of the laser beam. Positions measured in voltages were converted into displacements in nanometers by recording the time-dependent mean-square voltage $\langle \Delta V^2(\tau) \rangle$ of five particles from the same batch of particles, immediately before each set of measurements. Assuming the voltage recorded is proportional to the displacement, $\langle \Delta V^2(\tau) \rangle$ was fitted to the theoretical expression for the mean-squared displacement $\langle \Delta x^2(\tau) \rangle$ of a Brownian sphere in a harmonic potential, to yield the detector calibration and the optical trap stiffness k. In the optical torque experiments detailed in Sec. 4, the voltages from the four sections of each detector were summed together. Each of the two orthogonal detectors were separately calibrated so that they provided the power of each polarization component, in units of the power at the trap focus. The transmitted powers recorded by the x and y polarization detectors (P_x and P_y) were combined (see Section 4.1) to analyze the polarization change of the laser beam after it had passed through the nematic LC drop. Data was acquired by a Labview programme (National Instruments, Austin, Texas, USA) and digitized using a high-speed data acquisition card (National Instruments model PCI-MI0-16E-1).

3. Measurement of the charge on a single microparticle

Many key properties of colloidal suspensions are directly or indirectly controlled by the electrical charge carried by their constituent particles. Consequently, methods to measure the electrophoretic mobilities of colloidal particles have received a lot of attention during the last couple of decades. Most techniques available today, however, rely on ensemble averages and are based on monitoring the linear motion of particles in an electric field. Laser Doppler Velocimetry (LDV) is widely used[9] to investigate the light scattered by particles suspended in an electric field and to infer their charge, but is limited to large samples of monodisperse materials. Phase Analysis Light Scattering (PALS) is commonly used to measure very low particle charges in either non-polar suspensions[10] or near the isoelectric point but suffers from similar practical limitations to LDV. These methods, although fast and accurate, provide little or no information on the details of the charge distribution. In many cases, however, knowledge of the charge distribution is of vital importance. Colloidal suspensions have, for example, proved to be valuable model systems in condensed matter physics. There is strong evidence that the width of the charge distribution (the charge polydispersity) significantly influences the glass transition and at high levels may suppress the freezing transition in these systems.[11] It is therefore important that techniques are available that provide an accurate characterization of the charge distribution of microparticles.

Here, we report the development of an ultra-sensitive technique for the measurement of the charge carried by a *single* colloidal particle in a non-polar suspension. Our approach is to use the well-known phenomenon of the resonance of a harmonic oscillator driven by a oscillatory linear force. A linearly-polarized laser beam is used to trap a single microparticle. The laser and trapped particle constitute a harmonic oscillator with a stiffness that is proportional to the laser power. The modulation of the Brownian motion generated by an alternating electric field is measured with nanometer sensitivity using an interferometric position detector and the charge is

Published on 16 July 2007. Downloaded by University of Edinburgh on 01/11/2013 20:16:05.

 This journal is © The Royal Society of Chemistry 2007

View Article Online

obtained directly from the power spectrum of the thermal fluctuations. Charges as low as a few elementary charges can be measured with an uncertainty of about 0.25 e.[12] This is significantly better than existing techniques and opens up new possibilities for the study of non-polar suspensions.

3.1 Experimental details

We use a model colloidal system of sterically-stabilized poly(methyl methacrylate) spheres [PMMA] of radius $a = 610 \pm 30$ nm.[13] Electron microscopy revealed the particles were highly uniform in size with a radius polydispersity (root mean square variation/mean radius) of 0.046. Single PMMA spheres were suspended in dry dodecane and trapped in three dimensions using a linearly-polarized laser beam in a purpose-built microelectrophoresis cell. The cell contained two flat platinum foil electrodes separated by 128 μm ± 2 μm in a cylindrical glass sample chamber. Voltages of up to 10 V were applied to the electrodes. The electric field was estimated from the expression $E = \lambda V/d$, where V is the applied voltage, d is the plate separation and, λ is a factor correcting for the finite size of the electrodes. Finite element simulation of the electric field gave $\lambda = 0.93$. The confined microparticle was held about 70 μm above the base of the cell and 2^{18} data points were collected at 10 kHz. The Brownian motion of the particle was followed by back-plane optical interferometry using data collected from just one quadrant photodetector. The duration of each measurement was ≈26 s.

3.2 Brownian motion of an oscillating microparticle

The total force on a *charged* microparticle in an optical trap has four elements: a harmonic force, $-kx(t)$, arising from the optical trap, where k is the force constant of the potential well; a viscous drag force $-\xi_t\dot{x}(t)$, where from Stokes law $\xi_t = 6\pi\eta a$ for a sphere of radius a; an oscillatory driving force $f_D(t) = A \sin \Omega t$ defined by the frequency Ω and amplitude A of the applied electric field; and Brownian forces $f_B(t)$ characterizing the random fluctuating forces due to collisions with molecules of the solvent. The Langevin force equation for the Brownian motion of a sphere of mass m is,[14]

$$m\ddot{x} = -kx - \xi_t\dot{x} + A \sin \Omega t + f_B(t) \tag{6}$$

where $f_B(t)$ is a white-noise Gaussian random process with time-averaged correlations $\langle f_B(t)\, f_B(t')\rangle = 2\xi_t k_B T\delta(t - t')$. To simplify the problem, we neglect all inertial terms that are negligible at frequencies $\omega \ll 10^6$ rad s^{-1}. Defining the amplitude of the oscillatory linear force as $A = ZeE$, where Z is the charge on the microparticle and E is the amplitude of the electric field, then eqn (6) reduces to

$$\xi_t\dot{x} + kx - ZeE \sin \Omega t = f_B(t). \tag{7}$$

Since the Brownian and periodic forces are uncorrelated, the general solution of eqn (7) is the superposition,

$$x(t) = x_B(t) + x_D(t), \tag{8}$$

where x_B is the solution in the presence of random Brownian forces *only* (*i.e.* $A = 0$) and x_D is the solution where only driven forces act (*i.e.* $T = 0$). The factorization evident in eqn (8) is universal, so, for instance, the spectral density $S_D(\omega)$ of the particle's positional fluctuations is simply a combination of the spectral densities for purely Brownian and driven motion,

$$S_D(\omega) = \frac{k_B T}{\pi\xi_t}\frac{1}{\omega^2 + \Omega^2} + \frac{k_B T\gamma^2}{2k}[\delta(\omega - \Omega) + \delta(\omega + \Omega)]. \tag{9}$$

Published on 16 July 2007. Downloaded by University of Edinburgh on 01/11/2013 20:16:05.

View Article Online

Here, we have introduced γ^2, the ratio of the mean-square driven and Brownian forces,

$$\gamma^2 = \frac{\langle f_D^2 \rangle / \langle f_B^2 \rangle}{1 + (\Omega/\omega_c)^2} \tag{10}$$

and the corner frequency of the potential well, $\omega_c = k/\xi_t$. The mean square amplitude of the driven forces is $\langle f_D^2 \rangle = Z^2 e^2 E^2/2$ while the mean square modulus of the fluctuating Brownian forces in a harmonic oscillator is $\langle f_B^2 \rangle = k_B T k$. The force ratio γ appears naturally in the theory and, as we show below, is also the quantity most readily extracted from experiment. In the weak-field limit, where $\gamma \ll 1$, the motion of the trapped microparticle is dominated by random Brownian forces. By contrast, in the strong-field limit where $\gamma \gg 1$, the thermal forces are only a relatively small perturbation and the oscillatory electrical forces dominate.

The experimentally measured spectral density of the Brownian fluctuations are plotted in Fig. 2 at different driving frequencies. The measured spectra are particularly simple, being a superposition of a Lorentzian spectrum (shown by the solid line) reflecting diffusive motion in a harmonic potential and a single δ-peak (arrowed) at the fundamental electrode drive frequency Ω. The data contains no higher harmonics of Ω, confirming the linear response of particle and field. To extract the power in the periodic signal, the data around the δ-spike was masked and the diffusive spectrum fitted to the first term of eqn (9), by adjusting the unknown corner frequency ω_c. Subtracting the fitted Lorentzian from the measured power spectra yielded the signal spectrum. The mean-square displacement P_{sig} of the microparticle in the electric field was obtained by integrating the signal spectrum around the peak at $\omega = \Omega$. From eqn (9),

$$P_{sig} = \frac{k_B T}{k} \gamma^2. \tag{11}$$

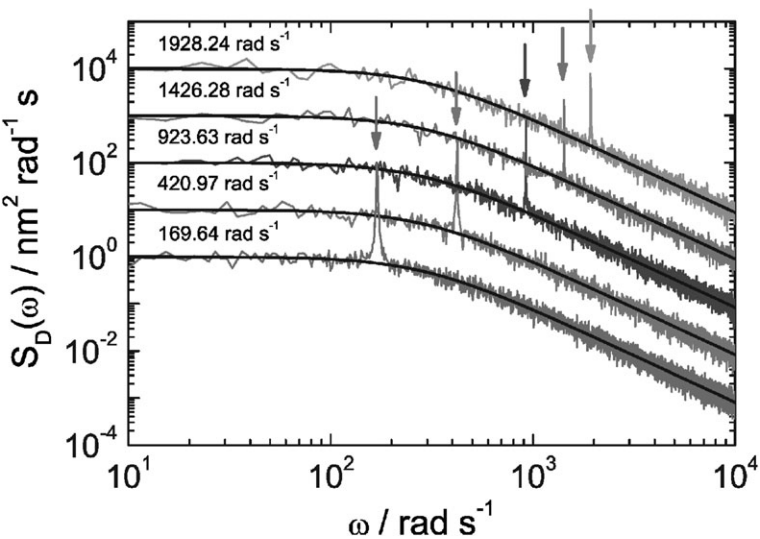

Fig. 2 The frequency dependence of the power spectral density $S_D(\omega)$. The sample was a 610 nm PMMA particle suspended in dodecane with 0.035 wt% added PHSA-g-PMMA copolymer. The amplitude of the electric field was fixed at $E = 72.8$ kV m^{-1} and the field frequency Ω varied. The arrows indicate the oscillatory fluctuations generated by the applied field.

 This journal is © The Royal Society of Chemistry 2007

Published on 16 July 2007. Downloaded by University of Edinburgh on 01/11/2013 20:16:05.

View Article Online

so a measurement of P_{sig} yields directly an estimate of the force ratio γ. An expression for the charge on the trapped microparticle follows immediately from eqn (10) and (11) as,

$$(Ze)^2 = \left[\frac{2\xi_t^2(\Omega^2 + \omega_c^2)}{E^2}\right] P_{sig}. \quad (12)$$

At low driving frequencies $\Omega \ll \omega_c$ this result simplifies to

$$(Ze)^2 = 2(k/E)^2 P_{sig}. \quad (13)$$

Published on 16 July 2007. Downloaded by University of Edinburgh on 01/11/2013 20:16:05.

3.3 Applications

The optical tweezers technique, detailed above, for the measurement of charge on individual microparticles has several advantages over existing methods. First, the approach is capable of very high sensitivity. Second, the measurements can be made rapidly, and third, the measurements are accurate and reproducible. We illustrate these benefits with two examples.

Fig. 3 show the effect of adding the surfactant sodium bis(2-ethylhexyl) sulfosuccinate [Na-AOT] to dilute PMMA suspensions in dry dodecane. At low concentrations c_s of Na-AOT ($c_s < 0.1$ mM), the particles have a very small residual charge. Attempts to measure the level of charge with a commercial PALS instrument were unsuccessful—the charge was below the detectable limit for this technique and the particle was incorrectly identified as having no charge. The low particle mobilities, however, presented no problems for the optical tweezers measurements, as the data in Fig. 3 confirms. The mean charge was measured as -2.9 ± 0.2 e. Increasing the concentration of surfactant results in the particle developing a large negative charge of $\langle Z \rangle \sim -50$ e. While such micelle-mediated charging has been known for at least the last 60 years,[15] the exact mechanism of charging in non-polar media has remained problematic and is not well understood. Recent work has highlighted the growing importance of charge in non-polar suspensions[16] and its technological significance.[17] The data of Fig. 3 reveals that our method is capable of accurate and reliable measurements of the extremely low level of particle charges characteristic of non-polar suspensions. Such improvements in quantitative characterization are an

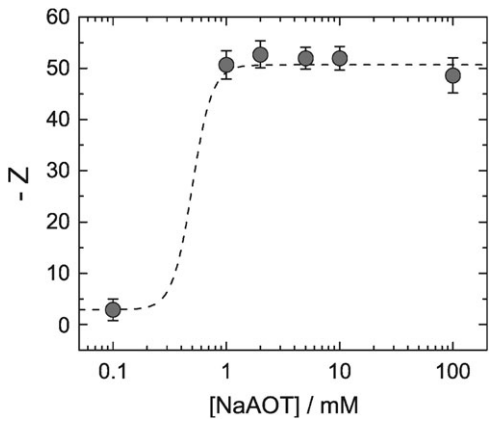

Fig. 3 The charge Z (in units of e) on undyed PMMA microspheres in dry dodecane as a function of AOT concentration. The error bars depict the variation in the charge of different particles under the same conditions. The uncertainty in Z from measurements on a single particle is significantly smaller.

View Article Online

Published on 16 July 2007. Downloaded by University of Edinburgh on 01/11/2013 20:16:05.

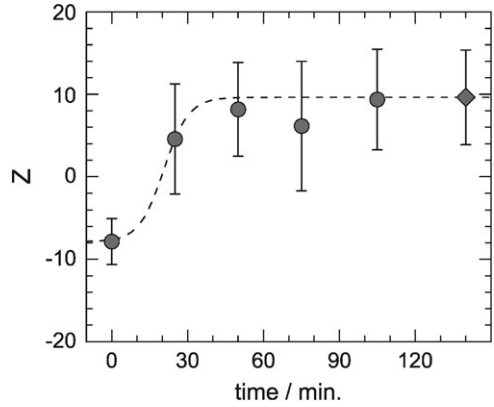

Fig. 4 Charge inversion caused by adsorption of water. The charge Z (in units of e) of dyed PMMA spheres in dry dodecane is plotted as a function of the exposure time (circles). The diamond indicates the limiting charge where the dispersion was left overnight in contact with excess water.

essential first step to developing a more detailed understanding of the role of charge in non-polar suspensions.

The small particle charges frequently found in non-polar suspensions means the level of charge is very sensitive to low concentrations of any surface-sensitive impurities. So, for instance, there have been several, and sometimes contradictory, reports in the literature[15] of the role of small amounts of water on the particle charge level. A key requirement for any technique used to investigate such an effect is rapidity of measurement. Fig. 4 reveals the speed capabilities of the optical tweezers technique, where reproducible measurements on single microspheres can be achieved within $\sim$30 s. Poly(methyl methacrylate) spheres containing the cationic dye $DiIC_{18}$ were suspended in dodecane, which had been carefully dried with activated molecular sieves (Acros, size 4A) and stored under dry nitrogen. The charge on the particle was followed as the dispersion was exposed for progressively longer periods to a damp atmosphere. The data in Fig. 4 shows the results. While initially the dyed particles are negative with a charge of about -8 e, the charge starts to reduce immediately on initial exposure to water, reversing its sign within 30 min and saturating at $+10$ e after $\sim$50 min.

4. Measurement of optical birefringence

The transfer of angular momentum from a light beam to a micron-sized particle by optical tweezers has become an important tool for the manipulation and characterization of objects in nanoscience.[18] The major application of this technique has been the study of microscopic biological systems. Microspheres have been used as a handle to rotate biological structures and to measure the associated torque. Other uses have emerged in the field of microfluidics, where optically-driven particles have been used as miniaturized pumps and stirrers[19] and as quantitative probes of rheological properties in microscopic volumes.[20] Quantitative applications depend on an accurate knowledge of the optical properties of the microparticles used. Here, we report on the birefringence of liquid crystal droplets dispersed in water. Previous work has shown that the internal molecular alignment of a liquid crystal is very sensitive to the local environment of the droplet.[21,22] So, for instance, the alignment of nematic LC drops may be changed from bipolar to radial by adding a surfactant. The coupling between rotating particle and fluid is, to date, little understood and difficult to probe. We demonstrate an optical technique that can accurately measure the *in situ* birefringence of a rotating probe particle. These measurements allow

 This journal is © The Royal Society of Chemistry 2007

View Article Online

the effect of the local environment on the molecular alignment to be quantified directly.

Two nematic liquid crystals were used in our experiments. MLC-6815 from Merck is a positive uniaxial birefringent material, with $n_o = \sqrt{1+\chi_o} = 1.444$ and $n_e = \sqrt{1+\chi_e} = 1.495$ while MDA-00-1444 has $n_o = 1.484$ and $n_e = 1.661$ at $\lambda = 1064$ nm. Both liquid crystals are hydrophobic so when dispersed in deionised water they naturally forms spherical drops with a dipolar alignment. The droplets have a distribution of radii a of between 0.5–5 μm. The sample was prepared by encasing the dispersion within a 10 mm wide hole in a 500 μm thick glass slide between two glass coverslips. Captured in a circularly-polarized light beam a droplet spins continuously. To measure the optical anisotropy of the birefringent droplet the fluctuations in the intensity of the elliptically polarized outgoing beam exiting the rotating drop were measured using the two orthogonal quadrant photodetectors, shown in Fig. 1. In order to determine the birefringence of the spinning LC droplet, we have to analyze the change in the polarization of the laser trap illumination after it has passed through the droplet.

Published on 16 July 2007. Downloaded by University of Edinburgh on 01/11/2013 20:16:05.

4.1 Angular momentum transfer

The oscillating electric field **E** of a monochromatic plane wave may be described in terms of the superposition of two orthogonal components,

$$\mathbf{E} = (E_x\hat{\mathbf{x}} + E_y\hat{\mathbf{y}}) \exp(ikz - i\omega t) \tag{14}$$

where the wave is propagating in the z-direction and ω, k are the angular frequency and wavevector of the beam, respectively. Since in general an incident beam will be elliptically polarized, that is it contains both circularly polarized and linearly polarized components, the amplitudes E_x and E_y will be complex. In the special case of circularly polarized light, where $E_y = \pm iE_x$, the total electric field has a constant magnitude and a field direction that rotates around the z-axis with the optical frequency ω. The sign depends on whether the beam is left (+) or right (−) circularly polarized. The spin angular momentum of left and right circularly polarized photons is $\pm\hbar$,[23] so that the flux of angular momentum in a circularly polarized light beam of power P is $\pm P/\omega$.[24,25]

The spin angular momentum carried by a general light beam may be readily calculated from the amplitudes of the equivalent left and right circular components of the electric field,

$$\begin{aligned} E_L &= \frac{1}{\sqrt{2}}(E_x - iE_y) \\ E_R &= \frac{1}{\sqrt{2}}(E_x + iE_y). \end{aligned} \tag{15}$$

The polarization coefficient,

$$\sigma = \frac{E_L^* E_L - E_R^* E_R}{E_L^* E_L + E_R^* E_R} = (P_L - P_R)/P \tag{16}$$

summarizes the state of polarization of a general beam, where P_L and P_R are the powers of the two orthogonal circularly-polarized components and P is the total power. A left circularly polarized beam has $\sigma = 1$. The spin angular momentum flux of the beam is accordingly,[25]

$$L = \sigma P/\omega. \tag{17}$$

In general, if the trapped material is birefringent then the polarization state of the illuminating laser beam will change after it has passed through the droplet and the angular momentum of the emerging beam will differ from that of the illuminating beam. To conserve the total angular momentum of the system, momentum must be

View Article Online

transferred to the birefringent particle and a torque on the particle will result. In the particular case where the illuminating beam is purely left circularly-polarized ($\sigma_{in} = 1$) and the emerging beam has the polarization σ_{out}, then the reaction torque on the particle will equal the loss of the angular momentum flux of the light beam,

$$\tau = (1 - \sigma_{out})\frac{P}{\omega}\hat{\mathbf{z}}. \tag{18}$$

Published on 16 July 2007. Downloaded by University of Edinburgh on 01/11/2013 20:16:05.

The amplitude of the reaction torque is a maximum when the birefringent microsphere acts as a $\lambda/2$-plate, so that the handedness of the emerging light beam is totally reversed and $\sigma_{out} = -1$.

The polarization coefficient of the emerging trapping beam σ_{out} was determined directly from the total voltage recorded by the two orthogonal quadrant photodetectors. The power of the left and right hand circularly-polarized components of the emerging beam are $P_L = (1 + \sigma_{out})P/2$ and $P_R = (1 - \sigma_{out})P/2$, respectively. Rewriting these components in terms of the electric fields along the lab-fixed x- and y-axes it is straightforward to show that the transmitted power measured, after the polarized beam splitter, by the two orthogonal quadrant detectors is

$$P_{x,y}(t) = \left(1 \pm \sqrt{1 - \sigma_{out}^2}\sin 2\theta\right)\frac{P}{2}, \tag{19}$$

where the positive sign is associated with the x-detector and θ is the angle between the optic axis of the liquid crystal and the lab-fixed x-axis. The reaction torque applied to the particle may be determined directly from the difference between the powers recorded on the two detectors scaled by the total beam power,

$$\mathscr{R}(t) = \frac{P_x(t) - P_y(t)}{P_x(t) + P_y(t)} = \sqrt{1 - \sigma_{out}^2}\sin 2\theta. \tag{20}$$

As the droplet rotates, the ratio $\mathscr{R}(t)$ alternates between maximum and minimum values of $\pm\sqrt{1 - \sigma_{out}^2}$, corresponding to orientations where the angle between the optic axis and the x-direction is $\theta = n\pi \pm \pi/4$. In between, where the optic axis of the birefringent droplet is parallel to the x-axis, $\mathscr{R}(t) = 0$. An example dataset of the $P_x(t)$ and $P_y(t)$ detector signals from a rotating LC droplet is shown in Fig. 5a and the corresponding ratio, $\mathscr{R}(t)$, in Fig. 5b. The extrema of $\mathscr{R}(t)$ following eqn (20) provide strictly only a measurement of the degree of circular polarization in the emerging beam $|\sigma_{out}|$ and not its direction (or sign). However, the sign of σ_{out} may be readily determined by inspection.

Measurement of the outgoing polarization σ_{out} and the beam power P gives an absolute measurement of the constant torque τ applied to the birefringent droplet, from eqn (18). The resulting droplet rotation rate Ω is determined from the Fourier

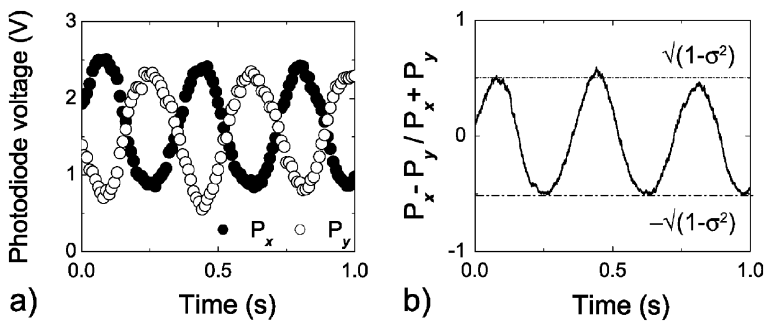

Fig. 5 Representative dataset showing (a) unnormalised P_x and P_y photodiode signals and, (b) the ratio $\mathscr{R}(t)$.

 This journal is © The Royal Society of Chemistry 2007

View Article Online

analysis detailed in Section 4.2. To establish the optical birefringence of the droplet, we assume that the liquid crystal acts as an ideal wave plate with a thickness equal to the diameter of the droplet, upon which a circularly polarized beam impinges at normal incidence. The polarization coefficient of the emerging beam is then $\sigma_{out} = \cos \Delta$, where the phase shift Δ between electric field components travelling parallel and normal to the optic axis of the liquid crystal is equal to,

$$\Delta = \frac{4\pi a \Delta n_{eff}}{\lambda} \tag{21}$$

with $\Delta n_{eff} = n_e - n_o$. The radius a of the LC droplet was measured by video microscopy and used together with the experimental value of σ_{out} to calculate the (effective) birefringence Δn_{eff} of the droplet.

4.2 Brownian motion of a rotating droplet

The normalized detector signal $\mathscr{R}(t)$ is sensitive to the instantaneous angular coordinate θ of the droplet. In this section, we exploit this dependence to study the rotational diffusion of a sphere driven by a constant torque.

The dynamics of the birefringent droplet is controlled by a balance of three contributions: a constant driving torque τ that arises from the transfer of angular momentum from the circularly polarized beam; a viscous drag torque $\xi_R\dot{\theta}$; and a white noise thermal torque $\tau_B(t)$ that represents the random torques imparted by thermal collision with the solvent molecules. The fluctuation dynamics of the droplet are governed by the Langevin torque equation,

$$I\ddot{\theta} = \tau - \xi_R\dot{\theta} + \tau_B(t), \tag{22}$$

where I is the moment of inertia of the droplet and ξ_R is the rotational friction coefficient, which for a sphere of radius a is, from Stokes law, $\xi_r = 8\pi\eta a^3$. The Brownian torques have a time-averaged mean value of zero and are delta correlated,

$$\langle \tau_B(t) \rangle = 0; \ \langle \tau_B(t)\tau_B(t') \rangle = 2\xi_R k_B T \delta(t' - t). \tag{23}$$

The spectral density of the random torque $C_B(\omega)$ is frequency independent,

$$C_B(\omega) = \frac{1}{2\pi}\int_{-\infty}^{+\infty} \langle \tau_B(t')\tau_B(t'+t) \rangle \exp(-i\omega t)\, dt = \frac{\xi_R k_B T}{\pi}. \tag{24}$$

The effect of a constant driving torque τ is to produce a uniform rotation of the droplet which modulates the correlation functions and leads to a subsequent resonance peak in the power spectrum. To understand these changes we consider first the rotational diffusion in the absence of a torque. In the limit of ordinary diffusion ($\tau = 0$), the solution of eqn (22) is obtained readily by Fourier techniques.[14] The Fourier transform of the angular correlation function, $C_{\theta\theta}(t - t') = \langle \theta(t)\theta(t') \rangle$, is

$$C_{\theta\theta}(\omega) = \frac{k_B T \xi_R}{\pi\omega^2[I^2\omega^2 + \xi_R^2]} \tag{25}$$

where we have used eqn (24). In the low frequency limit $\omega \ll \xi_R/I$, appropriate here since ξ_R/I is of order 10^7 rad s^{-1}, this expression reduces to the well-known inverse square spectrum:

$$C_{\theta\theta}(\omega) = \frac{k_B T}{\pi\omega^2 \xi_R}. \tag{26}$$

In the presence of a constant torque, the optic axis of the droplet is set spinning at a constant average rate. Neglecting the inertial terms, which are negligible at frequencies $\omega \ll \xi_R/I$ and averaging eqn (22) over the fluctuating Brownian torques reveals

Published on 16 July 2007. Downloaded by University of Edinburgh on 01/11/2013 20:16:05.

View Article Online

Published on 16 July 2007. Downloaded by University of Edinburgh on 01/11/2013 20:16:05.

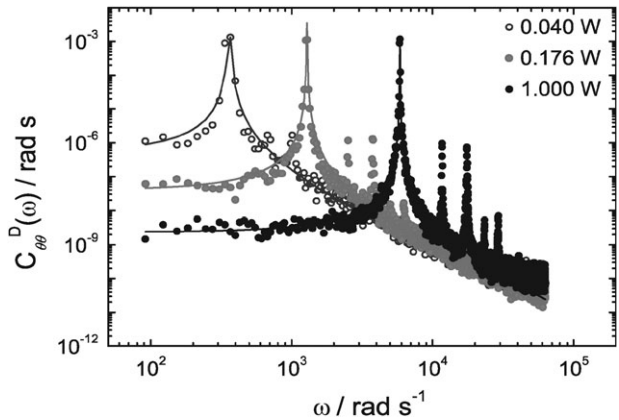

Fig. 6 The spectral density of the orientational fluctuations $C_{\theta\theta}^{D}(\omega)$ measured on a single spinning birefringent LC droplet (MDA-00-1444) of radius $a = 1.2$ μm with retardation $\Delta \sim 0.5$. The solid lines show fits of the measured spectral densities to eqn (29).

that the average rotation rate of the droplet is,

$$\langle \dot{\theta} \rangle = \frac{\tau}{\xi_R} = \Omega. \tag{27}$$

Although the average rotation rate is fixed at Ω, there remains fluctuations in the rotation rate due to collisions between the trapped drop and molecules of the solvent, which result in the application of additional random torques. Provided the time for rotation Ω^{-1} is longer than the characteristic relaxation time of the angular correlations of the droplet, then the effect of the continuous (non-Brownian) rotation is simply to modulate the purely diffusive angular correlation function $C_{\theta\theta}(t)$. The driven correlations $C_{\theta\theta}^{D}(t)$ will therefore, to a first approximation, have the form[26]

$$C_{\theta\theta}^{D}(t) = C_{\theta\theta}(t)\cos 2\Omega t, \tag{28}$$

where the periodic term arises from the non-random rotation and the factor of 2 is because the rotating linear component of light emerging from the droplet is parallel to each polarizer twice during a complete rotation of the droplet. The associated power spectrum exhibits a resonance at the frequency characteristic of the driving torque. Using the Fourier shift theorem and eqn (26)–(28), the spectral density of the angular fluctuations in the continuously driven droplet is,

$$C_{\theta\theta}^{D}(\omega) = \frac{k_B T}{\pi \xi_R (\omega - 2\Omega)^2} \tag{29}$$

In Fig. 6, we fit the power spectra measured from a single rotating drop at three different torques to eqn (29) and there is excellent agreement. At low frequencies, $\omega \ll \Omega$, eqn (29) saturates at a constant value, $C_{\theta\theta}^{D}(\omega)_{sat} = k_B T/4\pi\xi_R\Omega^2$, which is inversely proportional to the square of the driving frequency, as evident in Fig. 6. At high frequencies, $\omega \gg \Omega$, eqn (29) simplifies to $C_{\theta\theta}^{D}(\omega)_{sat} = k_B T/\pi\xi_R\omega^2$, indicating that diffusion dominates.

4.3 Applications

Detailed analysis of the orientational fluctuations show that the spinning liquid crystal droplets behave as mechanically rigid spheres. Fig. 7 shows that the rotation frequency Ω, obtained from the peak in the power spectra $C_{\theta\theta}^{D}(\omega)$, is a linear function of the laser beam power as expected from eqn (18) and (27). Similarly, the

 This journal is © The Royal Society of Chemistry 2007

View Article Online

Published on 16 July 2007. Downloaded by University of Edinburgh on 01/11/2013 20:16:05.

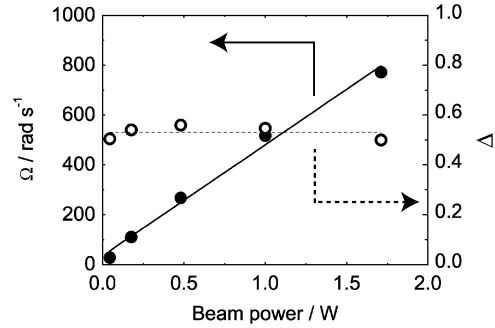

Fig. 7 The rotation frequency Ω (filled points) and phase shift Δ (open points) as a function of beam power (a = 1.2 μm, MDA-00-1444).

retardation Δ is constant, independent of the laser power, signifying that there is no change in internal molecular ordering or flow within the droplets for the powers typical of our experiments.

Accounting for the measured phase shift of the optical trapping beam as it passes through a nematic liquid crystalline droplet in terms of the birefringence of the material is not trivial. Within each droplet there is a range of molecular alignments. Whilst molecules near the centre of the droplet will be free to adopt the preferred dipolar orientation, surface energetics will favour parallel anchoring at the water interface. The competition between elastic deformation and anchoring energies define a continuous director field that is a function of the radial distance from the centre of the drop. As a result, the birefringence determined from the measured phase shift Δ (eqn (21)) will be an average over the complete director field within the drop and is likely to depend on the drop radius a. Fig. 8 summarizes the experimental data on the size dependence of the effective birefringence Δn_{eff} for droplets of MDA-00-1444. For comparison, the bulk birefringence of the liquid crystal is Δn = 0.177. Fig. 8 reveals that in large drops, $a > 2$ μm, Δn_{eff} saturates at a near size-independent limit of $\sim$0.12, approximately two-thirds of the bulk birefringence, whilst in small drops, $a < 2$ μm, the effective birefringence is significantly smaller, with $\Delta n_{\mathrm{eff}}/\Delta n \approx 0.34$. The size dependent birefringence indicates that the central region where the director alignment is uniform is significantly reduced in small droplets.

The effective birefringence of a droplet provides a clear indication of detrimental environmental factors. This is demonstrated by the data of Fig. 9, where light absorption causes progressive heating in an optical trap and the liquid crystal to switch from the nematic to the isotropic state. At the transition, a sharp drop in the

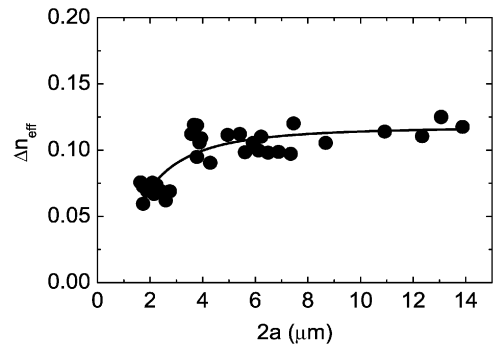

Fig. 8 The effective birefringence Δn_{eff} of nematic droplets of MDA-00-1444 as a function of diameter. The bulk birefringence is Δn = 0.177.

View Article Online

Published on 16 July 2007. Downloaded by University of Edinburgh on 01/11/2013 20:16:05.

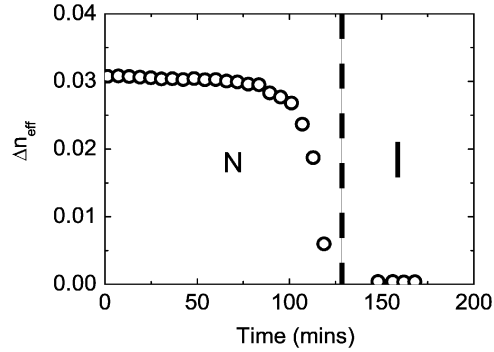

Fig. 9 Heating on prolonged irradiation. The birefringence Δn_{eff} reveals that, in a 4 W laser beam, heating destroys the nematic state after $\sim$2 h (a = 2.6 μm, MLC-6815).

effective birefringence of the droplet is observed, even though the particle still remains optically trapped. We can get an indication of the degree of heating by noting that MLC-6815 has a nematic-to-isotropic transition temperature of 67 °C. It is interesting to note that Fig. 9 reveals that in the nematic phase, $\Delta n_{eff} \sim 0.031$, which is approximately 60% of the bulk birefringence of MLC-6815, is in reasonably good agreement with the value obtained for the more birefringent MDA-00-1444. This consistency suggests that the effective birefringence of a spherical liquid crystal depends on the geometry of the system rather than any material property, and presents an interesting topic for further study.

5. Conclusions

The study of Brownian fluctuations in actively-driven situations provides new tools for the characterization of microparticles. In this manuscript, we have described two such examples. By using optical tweezers in combination with an external electric field, we have developed an ultra-sensitive method to measure the charge carried by an individual microparticle. The technique is fast, accurate and reproducible. Secondly, we have detailed how the application of a constant torque may be used to measure quantitatively the optical anisotropy of a spherical particle on a micron-scale. We anticipate that optical tweezers in combination with external fields will lead to further new techniques for particle characterization. Work in this direction is in progress.

Acknowledgements

We acknowledge financial support from the Engineering and Physical Sciences Research Council and Unilever PLC.

References

1 P. Riemann and P. Hanggi, *Appl. Phys. A*, 2002, **75**, 169.
2 L. Gammaitoni, P. Hänggi, P. Jung and F. Marchesoni, *Rev. Mod. Phys.*, 1998, **70**, 223.
3 Y. Roichman, V. Wong and D. G. Grier, *Phys. Rev. E*, 2007, **75**, 011407.
4 W. Denk and W. W. Webb, *Appl. Opt.*, 1990, **29**, 2382.
5 A. Ashkin, J. M. Driedzic, J. E. Bjorkholm and S. Chu, *Opt. Lett.*, 1986, **11**, 288.
6 P. Lorrain and D. Corson, *Electromagnetic Fields and Waves*, W. H. Freeman, San Francisco, 2nd edn, 1970.
7 P. Bartlett and D. Henderson, *J. Phys.: Condens. Matter*, 2002, **14**, 7757.
8 F. Gittes and C. F. Schmidt, *Opt. Lett.*, 1998, **23**, 7.
9 E. E. Uzgiris, *Adv. Colloid Interface Sci.*, 1981, **14**, 751.
10 J. F. Miller, K. Schatzel and B. Vincent, *J. Colloid Interface Sci.*, 1991, **143**, 532.
11 B. V. R. Tata and A. K. Arora, *J. Phys.: Condens. Matter*, 1995, **7**, 3817.

 This journal is © The Royal Society of Chemistry 2007

View Article Online

12 G. S. Roberts, T. A. Wood, W. J. Frith and P. Bartlett, *J. Chem. Phys.*, 2007, **126**, 194503.
13 L. Antl, J. W. Goodwin, R. D. Hill, R. H. Ottewill, S. M. Owens, S. Papworth and J. A. Waters, *Colloids Surf.*, 1986, **17**, 67.
14 R. Kubo, M. Toda and N. Hashitsume, *Statistical Physics II. Nonequilibrium statistical mechanics*, Springer Series in Solid-State Sciences, Springer-Verlag, Berlin, 1978.
15 I. D. Morrison, *Colloids Surf.*, 1993, **71**, 1.
16 M. E. Leunissen, C. G. Christova, A.-P. Hynninen, C. P. Royall, A. I. Campbell, A. Imhof, M. Dijkstra, R. v. Roij and A. v. Blaaderen, *Nature*, 2005, **437**, 235.
17 B. Comiskey, J. D. Albert, H. Yoshizawa and J. Jacobson, *Nature*, 1998, **394**, 253.
18 J. E. Molloy and M. J. Padgett, *Contemp. Phys.*, 2002, **43**, 241.
19 J. Leach, H. Mushfique, R. di Leonardo, M. Padgett and J. Cooper, *Lab Chip*, 2006, **6**, 735.
20 A. I. Bishop, T. A. Nieminen, N. R. Heckenberg and H. Rubinsztein-Dunlop, *Phys. Rev. Lett.*, 2004, **92**, 198104.
21 N. Murazawa, S. Juodkazis, S. Matsuo and H. Misawa, *Small*, 2005, **1**, 656.
22 N. Murazawa, S. Juodkazis and H. Misawa, *J. Phys. D*, 2005, **38**, 2923.
23 R. A. Beth, *Phys. Rev.*, 1936, **50**, 115.
24 M. E. J. Friese, T. A. Nieminen, N. R. Heckenberg and H. Rubinsztein-Dunlop, *Nature*, 1998, **394**, 348.
25 T. A. Nieminen, N. R. Heckenberg and H. Rubinsztein-Dunlop, *J. Mod. Opt.*, 2001, **48**, 405.
26 B. J. Berne and R. Pecora, *Dynamic Light Scattering with applications to chemistry, biology and physics*, John Wiley and Sons, New York, 1976.

Published on 16 July 2007. Downloaded by University of Edinburgh on 01/11/2013 20:16:05.